International Journal of Hybrid Information Technology
Vol.7, No.3 (2014), pp.275-284
http://dx.doi.org/10.14257/ijhit.2014.7.3.26

An Image Sub-pixel Edge Detection Algorithm of Plant Roots Based on Non-linear Fourth-order Interpolation Method

Wu Peng, Li Wenlin, Song Wenlong and Cao Jun*

College of Mechanical and Electronic Engineering, Northeast Forestry University, Harbin, 150040, China
wupengjacob@163.com

Abstract

To improve the accuracy of digital image edge detection, an ENO nonlinear fourth-order interpolation based subpixel edge detection algorithm was proposed in this paper. A stencil was constructed through classical Canny operator, followed by processing gray images to generate gradient images. ENO nonlinear fourth-order interpolation was applied in the gradient direction of target edges, and then subpixel subdivision computation was performed to obtain subpixel accurate locations of target edges, the performance of our edge detection algorithm was compared with that of centered cubic convolution and non-centered cubic convolution based edge detection methods. Simulation results demonstrated that the ENO based interpolation detection algorithm improved the abilities of detecting image edges.

Keywords: *edge detection; subpixel; ENO interpolation; Canny operators.*

1. Introduction

The process of edge detection is based on the hypothesis which directs that the edge is a point where the image intensity has sharp intensity transitions [1-3]. Important regions of interest are separated by different level of pixel intensity value. Upon this assumption, many edge detectors have been proposed. Most of them depend on the local pixel intensity gradient, done by differencing [4, 5] as a calculation of convolution of weighted matrix called local gradient mask. This group consists of well-known edge detector, such as Sobel, Roberts, Prewitt, Robinson, Kirsch [6,7]. Another interesting principle of edge detection [8,9] is done by approximation of circular masks and associating each image point with a local area of similar brightness. Their major drawbacks are high sensitivity to noise and disability to discriminate edges versus textures. Because of these limitations more advance edge detectors have been proposed which do not only detect edges but also try to connect neighboring edge points into a contour. In this way, many authors have developed different edge detectors based on the scale space [10, 11], active contours [12], morphological operations [13] and also gradient values [14]. Among all, the fundamental one is Canny edge detector [15], which is fast, reliable, robust and generic, but the accuracy is not satisfactory, because of the

ISSN: 1738-9968 IJHIT

parameters, which is the weakest point in the procedure. For this reason Canny was extended to the time-scale plane [16].

These operators detect image edges at the pixel level, but subpixel-level is required for edge detection in most applications. For example, precision of edge detection usually directly affects the accuracy of measurement in detecting micro physical factors of plant rhizosphere [17]. Therefore, it's meaningful to develop subpixel edge detection algorithms. Subpixel edge detection is to divide pixels around edges into subpixel for accurately locating edges. To estimate subpixel edges, three gray-level matrices were used [18]. A surface element model based on Laplace operator with Gaussian mask was proposed [19]. Zernike matrix and Sobel operators based subpixel edge detection algorithm was also developed [20]. A subpixel interpolation algorithm based on quadric polynomial least square fitting to approximate gradient was proposed [21]. A bilinear interpolation based method was used to increase image resolution, followed by obtaining fine grids as a prerequisite step of edge detections [22]. A covariance based adaptive interpolation method was used to reduce computational complexity [23], but large covariance matrix used in this method could generate errors. A weighted cubic convolution interpolation through local gradient was used to conserve intensity change [24].

In this paper, ENO （Essentially non-oscillatory） based nonlinear fourth-order interpolation and Canny operator was applied to detect edges of images. ENO interpolation algorithm was first introduced, and then ENO interpolation based subpixel edge detection algorithm was proposed. Simulation results demonstrated that the algorithm proprosed here could more accurately locate subpixel of edges, with abilities of edge thinning.

2. Description the Edge detection and ENO interpolation algotithm

2.1. Edge detection algorithm

The edge of an image is the area with the most useful information, containing discontinuous or even drastically changing gray scales. Edge extraction algorithms are operators which can detect pixels with edge features.

Classical edge detection algorithms include Laplacian、Roberts、Prewitt、Sobel、LOG、Canny operators, etc. [25]. Laplacian operator is quadric differential algorithm, and sensitive to noise. Robert operator can accurately locate edge, but sensitive to noise. Prewitt and Soble operators can refrain noise, but the accuracy of locating edge is not as good as Roberts operator. LOG operator first applied Gaussian function to smooth image, followed by using Laplacian operator to extract points crossing zero as edge. LOG operator could generate fake edges, with poor rejection to noise. In this paper, Canny operator was used, because of its good performance of detecting edges [26]. Canny operator used first order differential equation of Gaussian function, therefore obtaining a balance between noise rejection and edge detection.

2.2. ENO interpolation algorithm

ENO interpolation method selected polynomial stencil according to gray scale around every pixel, followed by estimating smoothness by calculating deviation from mean. ENO

interpolation selected interpolation points in self adaptive way. Although monotonicity couldn't be guaranteed, small shaking could be tolerated with high order accuracy [27].

Given a set of discrete values, $f_{ij} = f(x_i, y_j)$, which represent the pixel grey level value in a regular grid, where $x_i = x_{i-1} + d$, $y_i = y_{i-1} + d$, for each subpixel (x_*, y_*), a numerical interpolation is defined:

$$\begin{aligned} R(x_*, y_*; f) &= f(x_*, y_*) + O(d^4) \\ R(x_i, y_j; f) &= f_{ij} \end{aligned} \tag{1}$$

Where $O(d^4)$ is the definition of approximation error.

ENO interpolation method starts using a zero degree interpolation polynomial which coincides with the function value at one point (x_i, y_j). To obtain a higher order, another point should be added to the stencil, which is chosen from the two contiguous neighbors based on the lowest value of the two respective divided differences. This is an iterative process, carried out until the polynomial gets the desired order. The stencil selection is based on the use of divided differences as smoothness indicators [28]:

(A) Given $x_* \in [x_i - \frac{d}{2}, x_i + \frac{d}{2}]$, it is considered that $p_{i,k}(x_*; f)$ is the unique one-dimensional third-degree polynomial which interpolates the function $f(x, y_k)$ at the point $x = x_*$, using the stencil $\{x_{i_{\min k}}, x_{i_{\min k}+1}, x_{i_{\min k}+2}, x_{i_{\min k}+3}\}$ formed by 4 successive points that include x_i. The stencil is defined by the procedure described as follows:

(i) Initially, $i_{\min,k}^{(0)} = i$, $t_{i,k}^{(0)}(x_*; f) = f_{i,k}$;

(ii) For each $m \in \{1, 2, 3\}$, $i_{\min,k}^{(m-1)}$ and $t_{i,k}^{(m-1)}(x_*; f)$ are supposed to be known. Then the two following m-degree divided differences of the function $f(x, y_k)$ are computed as follows:

$$a_{i,k}^{(m)} = f\left\lfloor x_{i_{\min,k}}^{m-1}, x_{i_{\min,k}+1}^{m-1}, \ldots, x_{i_{\min,k}+m}^{m-1} \right\rfloor\Big|_{f=f_k} \tag{2}$$

$$b_{i,k}^{(m)} = f\left\lfloor x_{i_{\min,k}-1}^{m-1}, x_{i_{\min,k}}^{m-1}, \ldots, x_{i_{\min,k}+m-1}^{m-1} \right\rfloor\Big|_{f=f_k} \tag{3}$$

From the possible candidate points, the one with the lower divided difference value will be added to the stencil.

(a) if $\left|a_{i,k}^{(m)}\right| < \left|b_{i,k}^{(m)}\right|$, then: $c_{i,k}^{(m)} = a_{i,k}^{(m)}$, $i_{\min,k}^{m} = i_{\min,k}^{(m-1)}$,

(b) if $\left|a_{i,k}^{(m)}\right| > \left|b_{i,k}^{(m)}\right|$, then: $c_{i,k}^{(m)} = b_{i,k}^{(m)}$, $i_{\min,k}^{m} = i_{\min,k-1}^{(m-1)}$

Thus $p_{i,k}^{(m)}(x_*; f) = p_{i,k}^{(m-1)}(x_*; f) + c_{i,k}^{(m)} \prod_{j=i_{\min,k}^{(m-1)}}^{i_{\min,k}^{(m-1)}+m-1} (x_* - x_j)$,

and $i_{\min,k} = i_{\min,k}^{(3)}$, $p_{i,k}(x_*; f) = p_{i,k}^{(3)}(x_*; f)$.

(B) In the previous step(A), for each $x_* \in [x_i - \frac{d}{2}, x_i + \frac{d}{2}]$, a set of discrete values has been built, $p_{i,k}(x_*; f) \equiv p_{k,x}, \ \forall k = 1, \ldots, NY$.

Assuming that $y_* \in [y_j - \frac{d}{2}, y_j + \frac{d}{2}]$ and using the process described in the step (A), but the initial value is following:

$j^{(0)}_{\min, y_*} = j, \quad q^{(0)}_{i,y_*}(y_*; t) = t_{i,y_*}$, the following results in obtained after three interations:

$$q_{j,y_*}(y_*; t) = q^{(2)}_{j,y_*}(y_*; t) + c^{(3)}_{i,y_*} \prod_{k = j^{(2)}_{\min, y_*}}^{j^{(2)}_{\min, y_*} + 2} (y_* - y_k)$$

In the interpolation process a stencil has been used that is formed by four consecutive points including $y_j : \left\{ y_{j_{\min x_*}}, y_{j_{\min x_*+1}}, y_{j_{\min x_*+2}}, y_{j_{\min x_*+3}} \right\}$.

Thus, the stencil can be defined as $R(x_*, y_*; f) = q_{j,x_*}(y_*; t)$.

3. ENO interpolation based subpixel edge detection

3.1. ENO based non-linear fourth-order interpolation algorithm

The pixel values of digital image are acquired as a weighted average of the luminosity of a portion of the scene. Therefore, the approach considers that the pixels of an image represent the averages of a function $f(x, y)$:

$$\bar{f}_{i,j} = \frac{1}{d^2} \int_{y_j - \frac{d}{2}}^{y_j + \frac{d}{2}} \int_{x_i - \frac{d}{2}}^{x_i + \frac{d}{2}} f(x, y) dx dy \tag{4}$$

In the first step of the interpolation process, the resolution is increased by dividing the original pixel into four new pixel. Pixel values in the interpolated image will also be averages of the same function. Thus, the four average values can be computed from (5) to (8):

$$\bar{f}^{(1)}_{i,j} = \frac{1}{4d^2} \int_{y_j - \frac{d}{2}}^{y_j} \int_{x_i - \frac{d}{2}}^{x_i} f(x, y) dx dy \tag{5}$$

$$\bar{f}^{(2)}_{i,j} = \frac{1}{4d^2} \int_{y_j - \frac{d}{2}}^{y_j} \int_{x_i}^{x_i + \frac{d}{2}} f(x, y) dx dy \tag{6}$$

$$\bar{f}^{(3)}_{i,j} = \frac{1}{4d^2} \int_{y_j}^{y_j + \frac{d}{2}} \int_{x_i - \frac{d}{2}}^{x_i} f(x, y) dx dy \tag{7}$$

$$\bar{f}^{(4)}_{i,j} = \frac{1}{4d^2} \int_{y_j}^{y_j + \frac{d}{2}} \int_{x_i}^{x_i + \frac{d}{2}} f(x, y) dx dy \tag{8}$$

A Gaussian quadrature formula with four nodes is employed in order to compute these integrals with the desired local truncation error:

$$\bar{f}^{(1)}_{i,j} = \frac{1}{4d^2} \int_{y_j - \frac{d}{2}}^{y_j} \int_{x_i - \frac{d}{2}}^{x_i} f(x, y) dx dy \approx \frac{1}{4} [f(x_i - \frac{d}{2} + \beta, y_j - \beta) + f(x_i - \beta, y_j - \beta)$$

$$+ f(x_i - \frac{d}{2} + \beta, y_j - \frac{d}{2} + \beta) + f(x_i - \beta, y_j - \frac{d}{2} + \beta)] \quad (9)$$

$$\overline{\overline{f}}^{(2)}_{i,j} = \frac{1}{4d^2}\int_{y_j - \frac{d}{2}}^{y_j}\int_{x_i}^{x_i + \frac{d}{2}} f(x,y)dxdy \approx \frac{1}{4}[f(x_i + \beta, y_j - \beta) + f(x_i + \frac{d}{2} - \beta, y_j - \beta)$$

$$+ f(x_i + \beta, y_j - \frac{d}{2} + \beta) + f(x_i + \frac{d}{2} - \beta, y_j - \frac{d}{2} + \beta)] \quad (10)$$

$$\overline{\overline{f}}^{(3)}_{i,j} = \frac{1}{4d^2}\int_{y_j}^{y_j + \frac{d}{2}}\int_{x_i - \frac{d}{2}}^{x_i} f(x,y)dxdy \approx \frac{1}{4}[f(x_i - \frac{d}{2} + \beta, y_j + \frac{d}{2} - \beta)$$

$$+ f(x_i - \beta, y_j + \frac{d}{2} - \beta) + f(x_i - \frac{d}{2} + \beta, y_j + \beta) + f(x_i - \beta, y_j + \beta)] \quad (11)$$

$$\overline{\overline{f}}^{(4)}_{i,j} = \frac{1}{4d^2}\int_{y_j}^{y_j + \frac{d}{2}}\int_{x_i}^{x_i + \frac{d}{2}} f(x,y)dxdy \approx \frac{1}{4}[f(x_i + \beta, y_j + \frac{d}{2} - \beta)$$

$$+ f(x_i + \frac{d}{2} - \beta, y_j + \frac{d}{2} - \beta) + f(x_i + \beta, y_j + \beta) + f(x_i + \frac{d}{2} - \beta, y_j + \beta)] \quad (12)$$

Where $\beta = d(\frac{1 - 1/\sqrt{3}}{2})$. Therefore, the point values of $f(x_*, y_*)$ must be interpolated at the above quadrature nodes $(x_*, y_*) \in [x_i - \frac{d}{2}, x_i + \frac{d}{2}] \times [y_i - \frac{d}{2}, y_i + \frac{d}{2}]$.

According to [19]:

$\overline{\overline{f}}_j(x_*) = \frac{1}{d}\int_{-\frac{d}{2}}^{\frac{d}{2}} \overline{f}_j(x_* + \psi)d\psi$, being

$$\overline{f}_j(x_* + \psi) = \frac{1}{d}\int_{y_j - \frac{d}{2}}^{y_j + \frac{d}{2}} f_j(x_* + \psi, \varphi)d\varphi \quad (13)$$

A Taylor expansion of $\overline{f}_j(x_* + \psi)$ around $\psi = 0$ reveals the existence of constant, such as:

$$\overline{f}_j(x_*) = \overline{\overline{f}}_j(x_*) - \frac{1}{24}d^2\frac{\partial^2 \overline{\overline{f}}_j(x_*)}{\partial x^2} + O(d^4) \quad (14)$$

Beginning with the discrete values $\overline{\overline{f}}_{i,j}$, the procedure described in the step (A) (section 2), $\forall x_* \in [x_i - \frac{d}{2}, x_i + \frac{d}{2}]$, $\forall j \in \{1, \ldots, NY\}$, thus: $t_{i,j}(x_*; \overline{\overline{f}}) = \overline{\overline{f}}_{i,j}$, $\forall j = 1, \ldots, NY$, then:

$$\overline{f}_j(x_*) = t_{i,j}(x_*; \overline{\overline{f}}) - \frac{1}{24}d^2\frac{\partial^2 t_{i,j}(x_*; \overline{\overline{f}})}{\partial x^2} + O(d^4) \quad (15)$$

Given $x_* \in [x_i - \frac{d}{2}, x_i + \frac{d}{2}]$, considering (15) and applying the same procedure described in the step (B) (section 2), then:

$$R(x_*, y_*; \overline{\overline{f}}) = q_{j,x_*}(y_*; t) - \frac{1}{24} d^2 \frac{\partial^2 q_{i,x_*}(y_*; t)}{\partial y^2} \tag{16}$$

Type (16) can verify:

$$R(x_*, y_*; \overline{\overline{f}}) = f(x_*, y_*) + O(d^4) \tag{17}$$

Where $(x_*, y_*) \in [x_i - \frac{d}{2}, x_i + \frac{d}{2}] \times [y_i - \frac{d}{2}, y_i + \frac{d}{2}]$.

3.2. Sub-pixel Edge detection steps

The steps for ENO based subpixel edge detection method are as follows:

(a) Canny edge detection algorithm was applied to detect pixel edge of images, followed by extracting and saving edge information;

(b) ENO interpolation method was used to adjust the edge factors. Sixteen points were selected around every pixel, namely, $f(x_i - 3, y_j + 3)$、$f(x_i - 3, y_j - 3)$、$f(x_i + 3, y_j - 3)$、$f(x_i + 3, y_j - 3)$、$f(x_i - 1, y_j - 3)$、$f(x_i - 1, y_j + 3)$、$f(x_i + 1, y_j - 3)$、$f(x_i +, y_j + 3)$、$f(x_i - 3, y_j + 1)$、$f(x_i - 3, y_j - 1)$、$f(x_i + 3, y_j - 1)$、$f(x_i + 3, y_j + 1)$、$f(x_i - 1, y_j - 1)$、$f(x_i - 1, y_j + 1)$、$f(x_i + 1, y_j - 1)$、$f(x_i + 1, y_j + 1)$。

which were then applied to formula (9)、(10)、(11)and(12)to generate interpolation results. The points were selected according to method used in literature [29];

(c) Subpixel edge was generated by interpolation in step (b).

4. Simulation

To explore the utility and demonstrate the efficiency of the proposed subpixel edge detection algorithm, computer experiments on gray-level images are carried out. Figure 1 (including (a) and (b)) is the ideal image of plant roots.

The computer experiments are conducted to test the proposed algorithm. The experiments are designed to compare the ability of the proposed method on extracting sub-pixel edges from the plant roots image with centered cubic convolution interpolation method (algorithm 1) and non-centered cubic convolution interpolation method (algorithm 2).

Figure 1. The original root image

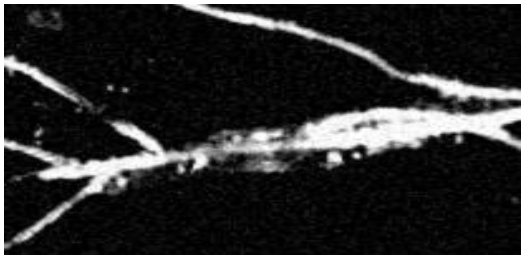

Figure 2. Algorithm 1

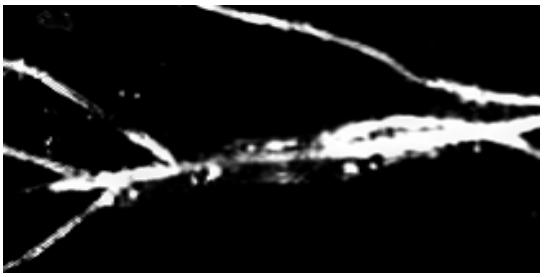

Figure 3. Algorithm 2

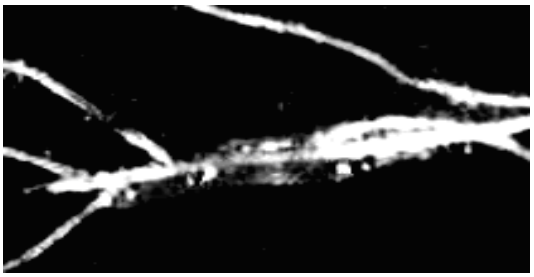

Figure 4. The algorithm proposed in this paper

Figure 2 - 4 show part of plant root image generated by edge detection. In Figure 2, the edge was blurry, because the image was made by centered cubic convolution interpolation edge detection algorithm which couldn't interpolate discontinuously. In Figure 3, the non-centered cubic convolution interpolation method was applied. Smoothing effect could be observed, but it's visually blurry. In Figure 4, our method was used. The image was clear and smoothing with good detection effects. Because ENO based interpolation detection method could perform better in conserving the geometrical features of image edge due to its uniform response, as a result, it improved the abilities of edge detection.

Because the quadric derivative of image edges is zero-cross, the convergence rates of quadric derivatives can be used as the relative accuracy for edges detected by different interpolation algorithms. For centered cubic convolution interpolation, $g_f''(x) = f''(x) - f''(x_i) + {2c_2}/{a^2} + O(d)$, which indicates that error increases, as d decreases. For non-centered cubic convolution interpolation, $g_c''(x) = f''(x) + O(d)$, which means the speed that quadric derivative error converges to zero is at least the same as that d decreasing to zero[30]. From formula (17), the speed that error decreases to zero in our algorithm is faster than that d decreasing to zero Therefore, in regards to convergence rate, the detecting accuracies of the three algorithms compared here from high to low were our algorithm, non-centered cubic convolution interpolation, and centered cubic convolution interpolation.

Given an image, different sampling rate were applied to obtain images with resolutions of 32×32 and 64×64 . The subpixel edges with different precisions were respectively compared with the baseline edge images generated by canny operator convolution. The larger the detection rate is, the higher the accuracy is. Table 1 is the comparison of accuracy of subpixel edges obtained by the three different subpixel edge detection algorithms.

Table 1. The rate of subpixel edge detection by three methods

	32×32	64×64
Algorithm 1	55.82	40.12
Algorithm 2	57.31	41.57
Proposed algorithm	59.62	43.65

From table 1, the detection accuracy of our method was higher than that of algorithm 1 and 2.

5. Conclusion

ENO based nonlinear fourth-order subpixel edge detection algorithm was proposed in this paper. ENO interpolation algorithm was first introduced, and then ENO based fourth-order interpolation algorithm was proposed. Our proposed method applied classical Canny operator for detecting image edges, followed by processing gray images to obtain gradient images. Based on the gradient images, ENO based fourth-order interpolation was performed along gradient direction of target edges for sub-division of subpixel by calculation to accurately locate target edges. The performance of our method was finally compared with that of centered cubic convolution interpolation-based or non-centered cubic convolution interpolation-based edge detection algorithm. The centered cubic convolution interpolation based edge detection method generated damages and blur effects for images to high extent. Non-centered cubic convolution interpolation based method made diffuse or smoothing effects. The simulation results demonstrated that our ENO based interpolation method performed better in conserving image dimensionality and direction, improving the abilities of image edge detection.

Acknowledgment

Fund Project: This paper is supported by the Fundamental Research Funds for the Central Universities (2572014CB14); this paper is supported by natural science foundation of Heilongjiang Province of China (C201337); this paper is supported by national natural science foundation of china (31270757).

References

[1] C. N. da Graaf and M. A. Viergever (Eds.), "Information Processing in Medical Imaging", Plenum Press, New Your, (**1988).**
[2] W. Niblack, "An Introduction to Digital Image Processing", Prentice Hall, Englewood Cliffs, NJ, (**1986).**
[3] J. Russ, "The Image Processing Handbook", Second ed., CDC Press, Boca Raton, (**1994).**
[4] A. Rosenfeld and A. Kak, "Digital Picture Proceesing", Academic Press, New York, (**1994**).
[5] M. Sonka, V. Hlavac and R. Boyle, "Image Processing, Analysis, and Machine Vision, Chapman and Hall, Cambridge, (**1993**).
[6] K. R. Castleman, "Digital Image Processing, Prentice-Hall, Upper Saddle River, (**1996).**
[7] D. Marr and E. Hildreth, "Theory of edge detection", Proc. R.Soc. Lond, (**1980**), pp.187-217.
[8] S. M. Smith, J. M. Brady, "SUSAN- a new approach to low lebel image processing", Int. J. Comput. Vision, (**1997**), pp. 45-78.
[9] J. Canny, "A Computational Approach to Edge Detection", IEEE Trans. Pattern Anal. Machine Intell, (**1986**), pp. 679-698.
[10] I. Laptev, H. Mayer and T. Lindeberg, "Automatic extrction of roads from aerial images based on scale-space and snakes", Mach. Vision Appl, (**2000**), pp. 23-31.
[11] P. Perona and J. Malik, "Scale space and edge detection using anisotropic diffusion", IEEE Trans. Patern Anal. Machine Intell. (**1989**), pp. 629-639.

[12] P. Meer and B. Georgescu, "Edge Detection with Embedded Confidence", IEEE Trans. Pattern Anal. Machine Intell, (**2001**), pp. 1351-1365.
[13] J. Li, "A Wavelet Approach to Edge Detection", Thesis, Sam Houston State University, (**2003).**
[14] I. Mikie, S. Krucinski and J. D. Thomas, "Segmentation and tracking in echocardiographic sequences-active contours guided by optical flow estimates", IEEE Trans. Medical Imaging, (**1998**), pp. 274-284.
[15] R. J. O'Callaghan and D. R. Bull, "Combined morphological-spectral unsupervised image segmentation", IEEE Trans. Image Process, (**2005**), pp. 49-62.
[16] P. Meer and B. Georgescu, "Edge Detection with Embedded Confidence", IEEE Trans. Pattern Anal. Machine Intell. (**2001**), pp. 1351-136.
[17] D. X. Hao, D. S. Xi and Y. Y. Yue, "Sub-pixel detection based on spatial moment and Zernike momnet [J]", Journal of Applied Scineces, (**2004**), vol. 22, no. 2, pp. 191-194.
[18] A. J. Tabatabai and O. R. Mitchell, "Edge location to subpixel values in digital imagery [J]", IEEE Transactions on Pattern Analysis and Machine Intelligence, (**1984)**, pp. 188-201.
[19] A. Huertas, "Detection of intensity changes with subpixel accuracy using laplacian guassian masks [J]", IEEE Transactions on Pattern Analysis and Machine Intelligence, (**1986**), pp. 651-664.
[20] S. Ghosal, "Orthogonal moment operators for subpixel edge-detection [J]", IEEE Transactions on Pattern Analysis and Machine Intelligence, (**1993),** pp. 295-306.
[21] F. Devernay, "A non-maxima suppression method for edge detection with subpixel accuracy [J]", IEEE Transactions on Pattern Analysis and Machine Intelligence, (**1995),** pp. 1-25.
[22] T. Kubota, T. Huntsberger and J. T. Martin, "Edge based probabilistic relaxation for subpixel contour extraction [J]", Image Vision Computing I, (**2001),** pp. 328-343.
[23] X. Li and M. T. Orchard, "New edge directed interpolation [J]", IEEE Transactions on Image Processing, (**2001**), pp. 1521-1527.
[24] J. W. Hwang and H. S. Lee, "Adaptive image interpolation based on local gradient features [J]", IEEE Signal Processing Letters, (**2004**), pp. 359-362.
[25] P. Eli, "Feature detection algorithm based on a visial ystem model [J]", Proceeding of IEEE, vol. 90 no. 1, (**2002**), pp. 78-94.
[26] J. Canny, "A computational approach to edge detection [J]", IEEE Trans Pattern Anal. Mach. Intell., vol. 6, (**1986**), pp. 679-698.
[27] A. Harten and B. Engquist, "Uniformly high order acdcurate non-oscillatory schemes [J]", I SIAM J Numer Anal, vol. 24, (**1987**), pp. 279-309.
[28] K. Siddiiqi and B. Kimia, "Geometric shock-capturing ENO schemes for subpixel interpolation [J]", Computation and curve evolution, Graphical Models and Image Processing, (**1997**), pp. 278-301.
[29] D. Su and P. Willis, "Image interpolation by pixel-level data-dependent triangulation [J]", Computers Graphics Forum, (**2004**), vol. 9, pp. 189-201.
[30] D. Su and P. Willis, "Image interpolation by pixel-level data-dependent triangulation [J]", Computers Graphics Forum, (**2004**), vol. 9, pp. 189-201.

